Orbital period modulation of the eclipsing binary system ER Vulpeculae: Real or not?

Alexandru Pop [a,*], Călin Vamoş [b]

[a] Romanian Academy, Astronomical Institute, Astronomical Observatory Cluj-Napoca, Str. Cireşilor 19, RO-400487 Cluj-Napoca, Romania
[b] Romanian Academy, "T. Popoviciu" Institute of Numerical Analysis, P.O. Box 68, 400110 Cluj-Napoca, Romania

A B S T R A C T

The reanalysis of the timing data of the binary system ER Vulpeculae revealed the superposition of a relatively slow increasing linear trend in the orbital period, having a relative period change rate of $2.73 \times 10^{-8}\,\mathrm{yr}^{-1}$, and a low amplitude ($\approx$3.5 min) periodic modulation with a period of about 17.78 yr. This periodicity is significantly shorter than that previously published, i.e., 30.6 yr. We propose a methodology relying on Monte Carlo simulations which is intended to evaluate the detectability of the inferred signal. Both frequentist and Bayesian approaches have been considered. The actual amplitude of the orbital period modulation might be lower than that obtained via nonlinear least-squares modelling of the timing data, namely about 2.0 min. Consequently, the amplitude of the underlying mechanism will be lower too. In the case of ER Vul, within the hypothesis of a third companion in the system, it could be a low mass star of about 113.8 $M_{Jupiter}$, but also a brown dwarf of about 64.7 $M_{Jupiter}$. Further theoretical and observational studies are needed in order to discriminate between this mechanism and the cyclic magnetic activity occurring in both component stars, as possible causes of the observed period variation.

1. Introduction

The eclipsing binary ER Vulpeculae (HIP 103833, HD 20039, BD+27°3952) is a detached, short-period, partially eclipsing system ($P \approx 0.6981$ d) consisting of two dwarf stars with spectral types G0 V + G5 V, according to Northcott and Bakos (1967), or G1–2 V + G3 V, according to Duemmler et al. (2003). It has been classified by Hall (1976) as a short-period RS CVn system (Ekmekçi et al., 2002; Çakirli et al., 2003; Duemmler et al., 2003; Kjurchieva et al., 2003; Shkolnik et al., 2005). Duemmler et al. (2003) argued that the system is still detached, although its primary component almost fills its Roche lobe. The spectroscopic studies performed by different authors evidenced the presence of circumstellar matter possibly resulted from mass loss phenomena from the stellar components (e.g., Kjurkchieva et al., 2003), or that of a broad, high-velocity stream of hot gas flowing onto the secondary component of the system (Shkolnik et al., 2005; see also Harmanec et al., 2004). Shkolnik et al. (2005) mentioned that the components of this system "*are the most chromospherically active solar-type stars known*" (Gunn and Doyle, 1997; Çakirli et al., 2003; Kjurchieva et al., 2003; see also references therein). Duemmler et al. (2003) confirmed the previous result of Gunn and Doyle (1997), that the secondary star is the most active component in the system. The light curve of ER Vul displays distortions and also variability phenomena at short-time scales (Mennella, 1990; İbanoğlu et al., 1993; Oláh et al., 1994; Kjurchieva et al., 2003; Harmanec et al., 2004). Dryomova et al. (2005) included ER Vul in their catalogue of DW-type eclipsing variable stars, which are pre-contact binary systems of short-periodic RS CVn-type evolving towards the W UMa type contact systems. In the SIMBAD database ER Vul is classified as an eclipsing binary of W UMa type. Both the observational features of the DW-type binary systems (e.g., Dryomova et al.,

2005), and intricate photometric and spectroscopic behaviour of ER Vul related to the intense chromospheric activity occurring in its component stars, make this system an interesting target for the investigation of the time behaviour of its orbital period.

The results of the available studies on the orbital period variation of ER Vul are relatively scarce and rather contradictory. Thus, Milano et al. (1986) and Mennella (1990) established parabolic ephemerides involving a period decrease and a period increase, respectively. Later, Qian et al. (1998) applied the method proposed by Kalimeris et al. (1994) with a fifth order polynomial model for the *O–C* curve. They inferred that the orbital period of ER Vul display a small amplitude modulation (0.32×10^{-5} d ≈ 0.28 s) with a periodicity of 30.6 yr superposed on a decreasing secular trend. Qian et al. (1998) and Qian (2001) assumed that the periodic modulation may be caused either by the cyclic magnetic activity in one or both components of the system, or by the presence of a very low-mass companion. They explained the secular period decrease of the orbital period of ER Vul through angular momentum loss via magnetic braking. Duemmler et al. (2003) argued that a parabolic model, corresponding to a period decrease, does not improve significantly the run of the *O–C* residuals with respect to a linear ephemeris. Moreover, they concluded that the orbital period of ER Vul did not display evidences for a change "*over at least 60 yr*" (see also Wilson and Raichur, 2011). Harmanec et al. (2004) established a new, improved linear ephemeris. The hypothesis of the constancy of the orbital period was adopted by them after performing some numerical tests. However, they did not exclude the possible presence of some "*mild variations of the orbital period*". Lastly, Liao and Qian (2010) considered that the available data on this system are inadequate for judgement of the character of its orbital period variation. Nanouris et al. (2011) suggested that in case of ER Vul the orbital period evolution could be mainly driven by the mass loss through stellar wind.

The main purpose of the present approach is to explore the presence of a low amplitude orbital period modulation in the binary system ER Vul, possibly embedded in the observational noise. Such a possibility is particularly interesting, having in view the spectral types of the two components and their intense chromospheric activity (Hall, 1989, 1990). Moreover, as it is well-known, Applegate's (1992) mechanism explains the orbital period modulation phenomena in active binary systems in which only the secondary component is chromospherically active (see also Lanza et al., 1998). Therefore, in case of ER Vul one could expect the coexistence of two orbital period modulation phenomena. On the other hand, according to the regression relationships obtained by us (Pop and Vamoş, 2012) reconsidering the correlation between the length of the activity cycle and the angular velocity emphasised by Lanza and Rodonò (1999) for active stars, we found for ER Vul a modulator period either of 27.9 yr or 26.6 yr. These values are obviously in good agreement with the periodicity of 30.6 yr found by Qian et al. (1998), although this periodicity has been proposed without a statistical substantiation, and its estimated amplitude is very low.

Because of the above mentioned contradictory results concerning the behaviour of the orbital period of ER Vul, and having in view the interest in clarifying the presence of a periodic modulation, we proposed in this study a methodology relying both on periodicity detection and *O–C* curve modelling, and on the evaluation of the detectability of the inferred periodic signal. The latter problem has been approached through decision-making, from both frequentist and Bayesian viewpoints (e.g., Appourchaux, 2011). In this context, we introduced the notion of signal detection probability, by extending the notion of trend detection probability previously defined by Pop et al. (2010). The final goal is to compare the effects of the null hypotheses H_0 (noise) and of the alternative hypothesis H_1 (periodic signal + noise) and to establish if their signatures would be perceived in the synthetic data through amplitude spectrum analysis. Finally, the astrophysical implications of the obtained results are discussed.

2. Observational data

The present study of the orbital period variation of the eclipsing binary system ER Vulpeculae relies only on photoelectric and CCD times of minimum light. We collected 92 primary minima and 78 secondary minima from the Lichtenknecker-Database of the BAV (http://www.bav-astro.de/LkDB) and "*O–C Gateway. Database of times of minima (E) and maxima (RR)*" of Variable Star Section of Czech Astronomical Society (http://var.astro.cz/ocgate/index.php), as well as the paper of Harmanec et al. (2004), and that of Samolyk (2012). The above data sets have been obtained after all timing data have been checked according to their original sources. During preliminary stages of data analysis we decided to reject several times of minimum light which were found to be outliers according to a $k\sigma$ criterion, where $k > 3$. Typical values of k used by us were: 5.0, 4.0, 3.5. This test has been applied in an iterative way. The Grubbs test was also used (see Pop and Bărbosu, 2006). The following primary minima have been rejected: 2435050.552 (Northcott and Bakos, 1956), 2444836.4751, 2444836.4758 (Pohl et al., 1982), 2445993.1749 (Srivastava et al., 1991), 2446265.46002 (Mennella, 1990), 2449563.24449 (Zeinali et al., 1995). We also rejected the U, B and V times of secondary minimum light at HJD 2449564 (Zeinali et al., 1995). The observed minima corresponding to the same event (eclipse) have been averaged. Thus, we got 48 primary minima and 44 secondary minima, which led us to a final data set consisting of 91 times of minimum light corresponding to distinct events (eclipses). They cover a time base of about 54.9 yr. The preliminary linear ephemeris has been obtained using the method proposed by Pop (1999) (see also Pop et al., 2003), followed by an improvement through linear regression $t_n = 2445221.10924(34) + 0.698094903(39)\,n$.

3. Data analysis methods

3.1. O–C curve modelling

In the present study on the orbital period variability of ER Vul, we applied the same methodology used in the previous papers of Pop et al. (2011) and Pop and Vamoş (2012) (see also the references therein). In the case of ER Vul, the timing data modelling through the classical *O–C* method relied on the following ephemeris (e.g., Pop et al., 2003)

$$t_n = t_0 + \tau_1 n + \tau_2 n^2 + \tau_{11} \sin(2\pi f_{01} n + \Phi_{11}), \quad j = 1, 2, \ldots, N_d, \tag{3.1}$$

in which the dimensionless frequency $f_{01} = P_p/P_{s1}$ ($P_p \equiv \tau_1$ being the orbital period, and P_{s1} the period of a possible periodic modulation of the orbital period) has been previously detected, while N_d is the number of analysed timing data. The periodicity detection was performed on the *O–C* residuals resulted after removing a parabolic secular trend, using the Monte Carlo type method previously reviewed by Pop et al. (2010) (see also Pop, 2005, 2007; Pop and Vamoş, 2007).

Note that for real data, the use of the Monte Carlo method for periodicity detection relying on $\tau_{\max}$ requires the preliminary data standardization. In fact, this procedure was already applied in case of Lomb–Scargle periodogram, in which the input data are transformed by removing their mean value, and then normalising by their standard deviation (e.g., Press and Rybicki, 1989).

We also applied – as a complementary method for time series analysis – the self-correlation method proposed by Percy et al.

(1981) (see also Percy et al., 1993; Percy et al., 2003). This method, which is conceptually different from that of amplitude spectrum analysis, is particularly useful because the influence of the magnetic activity on the orbital motion may be featured by the lack of strict periodicity (e.g., Applegate, 1992; Lanza et al., 1998).

3.2. Evaluation of the orbital period modulation detectability

It is well-known that in case of unevenly sampled data containing a periodic signal only, its amplitude spectrum will display a peak at the signal frequency. Because of spectral leakage (e.g., Deeming, 1975; Scargle, 1982) other peaks will occur at linear combinations between the signal frequency and the frequencies of the peaks appearing in the spectral window of the data. It is also well-known that in case of noisy data (e.g., consisting in pure Gaussian noise) the amplitude spectrum is also noisy (Scargle, 1982). Moreover, numerical simulations relying on Gaussian noise and the observed uneven data sampling revealed that the highest peak in the amplitude spectrum may occur at any frequency in the considered range, but with different probabilities [see Fig. 5 in Pop (2007), and Figs. 7 and 8 in Pop et al. (2010)]. In real situations, especially when we are dealing with a low amplitude periodic signal embedded in an additive noise with a relatively high level, our ability to detect such a signal through amplitude power spectrum analysis is determined by the interplay between the signal, the noise (its nature and level), and the spectral window of the available data. Sometimes, we also have to take into account an additional contribution, namely the unequal precision of individual observations.

Let us consider that we have detected the presence of a periodic signal (orbital period modulation phenomenon) in the analysed data, and that we have estimated the values of its parameters (frequency, amplitude, and phase) together with their corresponding standard errors: $f_{01} \pm \sigma(f_{01})$, $\tau_{11} \pm \sigma(\tau_{11})$, and $\Phi_{11} \pm \sigma(\Phi_{11})$. Let σ_{res} be the standard deviation of the residuals obtained after removing the periodic component (together with a possible secular trend). In order to estimate the detectability of the above periodic signal, we tested the null hypothesis H_0 (there is no signal in the data), and the alternate hypothesis H_1 (the data contain a well-defined periodic signal) by Monte Carlo simulations. We generated for each case N_{ex} artificial time series (O–C curves), with the time sampling of the original data, i.e., the cycle numbers of the observed timing data:

(i) N_{ex} data sets consisting of Gaussian noise with zero mean and σ_{res} standard deviation (H_0)

$$(O-C)(n_j;H_0) = \sigma_{res} N(0,1), \quad j = 1,2,\ldots,N_d, \tag{3.2}$$

(i) N_{ex} data sets consisting of a superposition of the above Gaussian noise over the inferred periodic signal (see Eq. (3.1)) (H_1)

$$(O-C)(n_j;H_1) = (O-C)(n_j;H_0) + k_\tau \tilde{\tau}_{11} \sin(2\pi \tilde{f}_{01} n_j + \tilde{\Phi}_{11}), \quad j = 1,2,\ldots,N_d, \tag{3.3}$$

in which the parameters of the periodic component are given by $\tilde{\xi} = \xi + \sigma(\xi)N(0,1)$, where ξ stands for τ_{11}, f_{01}, and Φ_{11}, while k_τ is a coefficient which allow us to control the signal's amplitude. Its role is to take into account the effect mentioned by Welsh (1997): superposing a Gaussian noise with different standard deviations over a sinusoidal signal with given amplitude and frequency, the amplitude estimated via least-squares method, ncreases as the amount of noise increases [see also the clean gain used by Roberts et al. (1987, p. 972) in the CLEAN Algorithm]. As it is expected, we found the same result for amplitudes estimated through amplitude spectrum computation.

Our approach to evaluate a given periodic signal in a well-defined observational context relies on the investigation, through Monte Carlo simulations, of two types of random processes occurring in the amplitude spectrum of synthetic data, in a given frequency range: (i) the occurrence of a particular value of a parameter which features the amplitude spectrum, and (ii) the frequency at which occurs the peak of a previously chosen rank in the amplitude spectrum. Hence, for each synthetic data set generated under the H_0 and H_1 hypotheses we computed the amplitude spectrum in the frequency range of interest. Finally, the amplitude spectra for H_0 and H_1 have been separately averaged. For each spectrum we estimated the values of the amplitude of the highest peak ($\tau_{\max}$), and the frequency of this peak in the amplitude spectrum.

Finally, we got the following information under both the H_0 and H_1 hypotheses: the distribution of $\tau_{\max}$, and the number of occurrences of the highest peak at a given frequency within the considered frequency range (N_{pj}, with $j = 0$ for H_0, and $j = 1$ for H_1). If f_{01}^* is the frequency at which the highest peak in the amplitude spectrum occurred most frequently, then let us call it the dominant frequency.

3.2.1. The frequentist approach

3.2.1.1. The decision-making relying on the τ_{max} distribution. Being given the distribution of $\tau_{\max}$ established under the H_0 and H_1 hypotheses, and its observed value $\tau_{\max,obs}$, let us denote: N_α – the number of $\tau_{\max}$ values under H_0 for which $\tau_{\max} > \tau_{\max,obs}$, and N_β – the number of $\tau_{\max}$ values under H_1 for which $\tau_{\max} < \tau_{\max,obs}$. The probabilities of committing a type I error (false alarm, false positive) and a type II error (false negative) are respectively

$$\alpha = N_\alpha / N_{ex}, \quad \beta = N_\beta / N_{ex}. \tag{3.4}$$

Obviously, the ideal situation occurs when $\alpha, \beta \to 0$.

3.2.1.2. The decision-making relying on the dominant frequency distribution. In this section we extended the notion of trend detection probability previously introduced by Pop et al. (2010) to the case of periodic signals. Within the frame of the "classical" approach, we are interested in the distribution of the amplitudes of the first order (highest) peak in the amplitude spectra of the artificial data sets generated under the H_0 and H_1 hypotheses. The idea of our approach is to estimate how often the first order peak in the amplitude spectrum (i.e., the signature of the periodic signal) occurs in the close proximity to the frequency of interest both under the H_0 and H_1 hypotheses. Our approach is justified in a natural way: the condition to be fulfilled in order to claim the detection of a periodic signal is the occurrence of the first order peak in the amplitude spectrum of the respective data approximately at the signal frequency. Thus, unlike the "classical" strategy which focuses on the amplitude information only, we take into account the amplitude information only by considering the peak order (the first order peak), but we also take into account the information concerning the position of the respective peak quantified by the corresponding frequency. From this view point the distribution value of the signal amplitude acquires a secondary importance for estimation of the signal detectability.

Let us assume that the highest peak in each of the N_{ex} amplitude spectra occurs most frequently at a frequency value f_{01}^* (the dominant frequency) situated in the immediate neighbourhood of the "observed"/detected frequency f_{01}. Let us also consider a frequency interval Δf_0 centred on f_{01}^*: $[f_{01}^* - \Delta f_0/2, \quad f_{01}^* + \Delta f_0/2]$. We define the signal detection probability under the hypothesis H_j ($j = 0, 1$), by means of the following formulae

$$\begin{aligned} P_{SD}(f_{01}^*, \Delta f_0; H_0) &= P_{SD}(H_0) = N_{p0}/N_{ex}, \\ P_{SD}(f_{01}^*, \Delta f_0; H_1) &= P_{SD}(H_1) = N_{p1}/N_{ex}. \end{aligned} \tag{3.5}$$

Concerning the choice of the frequency interval Δf_0, we may consider (as a maximum value) the frequency resolution corresponding to the available time base and time sampling, i.e., the width of the main peak (at zero dimensionless frequency) of the spectral window function (Δf_{0w}) (e.g., Deeming, 1975; Roberts et al., 1987).

According to the classification scheme given by Zwintz et al. (2000) and adapted by Pop et al. (2010) to the case of a linear trend, we may consider the following thresholds in order to give an interpretation of the results corresponding to the inferred periodic model and to a well defined observational context:

$P_{SD}(H_1) > 0.999$ – detectable signal,
$0.850 < P_{SD}(H_1) \leqslant 0.999$ – possible detectable signal,
$P_{SD}(H_0) < P_{SD}(H_1) \leqslant 0.850$ – signal difficult to be detected,
$P_{SD}(H_1) \leqslant P_{SD}(H_0)$ – undetectable signal.

In case of the null hypothesis H_0 we may distinguish the following thresholds:

$P_{SD}(H_0) > 0.999$ – spurious peak, false detection,
$0.850 < P_{SD}(H_0) \leqslant 0.999$ – possible spurious peak, possible false detection,
$P_{SD}(H_0) \leqslant 0.850$ – noisy peak.

3.2.2. The Bayesian approach

3.2.2.1. The decision-making relying on the τ_{max} distribution. For $\tau_{\max}$ values which satisfy the condition $\tau_{\max} \leqslant \tau_{\max,obs}$, we adopt the decision D_0, that the hypothesis H_0 is true, while in case of $\tau_{\max}$ values satisfying the condition $\tau_{\max} > \tau_{\max,obs}$, we adopt the decision D_1, that the hypothesis H_1 is true. In these conditions, using the Bayes theorem we can define the following four posterior probabilities for the two considered hypotheses (e.g., Liteanu and Rîcă, 1985; Axelsson, 1999; Fawcett, 2006)

$$P(H_i|D_j) = \frac{P(H_i)P(D_j|H_i)}{P(H_0)P(D_j|H_0) + P(H_1)P(D_j|H_1)}, \quad i,j = 0,1, \tag{3.6}$$

where $P(D_j|H_i)$ are the likelihoods of making the decision D_j, under the hypothesis H_i

$$\begin{aligned} &P(D_0|H_0) = 1-\alpha, \quad P(D_0|H_1) = \beta, \\ &P(D_1|H_0) = \alpha, \quad P(D_1|H_1) = 1-\beta, \end{aligned} \tag{3.7}$$

and $P(H_0) = P(H_1) = 1/2$ are the prior probabilities of the two considered hypotheses, about which we have no prior information about their relative importance (e.g., Sturrock and Scargle, 2009). Having in view our goal to evaluate the detectability of the inferred signal, we derived the following posterior probabilities, which can be expressed, using Eqs. (3.6) and (3.7), in terms of the probabilities to commit type I and type II errors, α and β, respectively

$$\begin{aligned} P(H_1|D_1) &= PPV = \frac{1-\beta}{1+\alpha-\beta}, \\ P(H_0|D_0) &= NPV = \frac{1-\alpha}{1-\alpha+\beta}, \end{aligned} \tag{3.8}$$

where *PPV* denotes the ***p**ositive **p**redictive **v**alue* (also called the Bayesian detection rate), which is the probability to obtain a $\tau_{\max}$ value, under the hypothesis H_1, which allow us to make the decision D_1, and *NPV* denotes the ***n**egative **p**redictive **v**alue*, which is the probability to obtain a $\tau_{\max}$ value, under the hypothesis H_0, which allow us to make the decision D_0. Obviously, a given parameter will have a higher performance in detectability evaluation, if both *PPV* and *NPV* values will be higher, tending ideally toward 100%.

3.2.2.2. The decision-making relying on the dominant frequency distribution. We also used the Bayes theorem in the form given by Eq. (3.6), in which the involved direct probabilities are expressed by the signal detection probabilities (see Eq. (3.5)) specific to the frequentist approach

$$\begin{aligned} &P(D_0|H_0) = 1 - P_{SD}(H_0), \quad P(D_0|H_1) = 1 - P_{SD}(H_1), \\ &P(D_1|H_0) = P_{SD}(H_0), \quad P(D_1|H_1) = P_{SD}(H_1). \end{aligned} \tag{3.9}$$

In these formulae, the data D_j ($j = 0, 1$) refers to the occurrences of the first order peak in the following spectral ranges: D_0 – the frequencies outside the considered interval $[f_{01}^* - \Delta f_0/2, f_{01}^* + \Delta f_0/2]$, D_1 – the frequencies inside the same interval. Because one has no prior information concerning the relative importance of H_0 and H_1, we considered $P(H_0) = P(H_1) = 1/2$. As in the previous case (Section 3.2.2.1) we will evaluate the detectability of the inferred signal using the previously defined posterior probabilities (3.8), taking into account the above formulae for the direct probabilities (Eq. (3.9))

$$\begin{aligned} P(H_1|D_1) &= PPV = \frac{P_{SD}(H_1)}{P_{SD}(H_0) + P_{SD}(H_1)}, \\ P(H_0|D_0) &= NPV = \frac{1 - P_{SD}(H_0)}{2 - P_{SD}(H_0) - P_{SD}(H_1)}. \end{aligned} \tag{3.10}$$

The above formulae allow us to find which of the two considered hypotheses is more likely to be true in the well-defined circumstances of our study. At the same time, we get quantitative information concerning our chance both to detect the inferred periodic signal when it is really present in the observed data, and to get a non-detection result when the inferred signal lacks from these data.

Finally, we emphasise that both posterior probabilities $P(H_1|D_1) = PPV$ defined by Eqs. (3.8) and (3.10), quantify our chance to detect the inferred signal, being given the sampling pathology of the observed time series (the *O–C* curve in our case), and the estimated noise level, assuming it to be of Gaussian character.

4. Results

4.1. O–C curve analysis and modelling

The *O–C* residuals of ER Vul proved to display a parabolic secular trend, the corresponding ephemeris being

$$t_n = 2445221.10773(46) + 0.698094938(36)n + 1.95(44) \times 10^{-11} n^2. \tag{4.1}$$

The relative period change rate is $(1/P_p)(dP_p/dt) = 2.93(65) \times 10^{-8}$ yr^{-1}, while the residuals standard deviation is $\sigma_{res} = 0.00291$ d.

The analysis of the *O–C* residuals obtained after removing the parabolic trend reveal the possible presence of a low amplitude (≈3.5 min) orbital period modulation with a periodicity of 17.78 yr (see Figs. 1 and 2, and Table 1). The statistical significance of the corresponding peak has been estimated using the Monte Carlo type method presented in Section 3.1 performing 100,000 numerical experiments. It supplied the following confidence levels for rejection null hypotheses built up using Gaussian noise, bootstrap resampling, and random permutation of the original data (keeping the original time sampling): 96.117%, 96.390%, and 96.361%, respectively. Such values suggest a moderately good argument to claim the detection of a signal, and thus they may be interpreted as a strong suspicion that we are dealing with a real periodicity buried in observational noise.

The self-correlation analysis of the above *O–C* residuals indicated the presence of a (quasi)periodicity of about 18.6 yr (Fig. 3). On the other hand, having in view the error bars of the first two deepest minima appearing in the self-correlation diagram (SCD), which occur at 18.5 yr and 37.5 yr (close to 2×18.5 yr), we may consider that, within the limits of the observational errors,

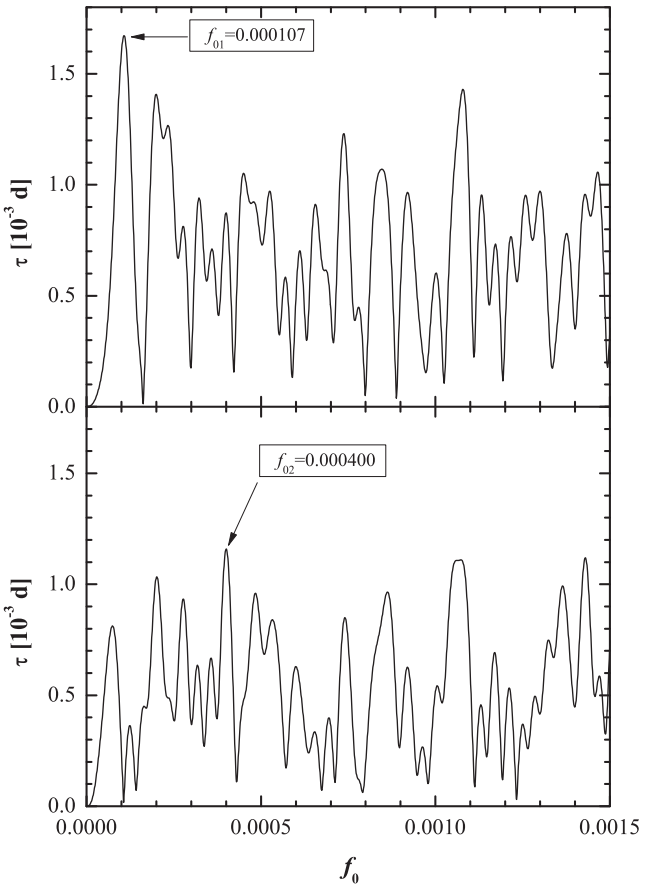

Fig. 1. Amplitude spectra of the *O–C* curve of ER Vul obtained after removing the parabolic trend (upper panel), and the parabolic trend + the inferred periodic signal (lower panel).

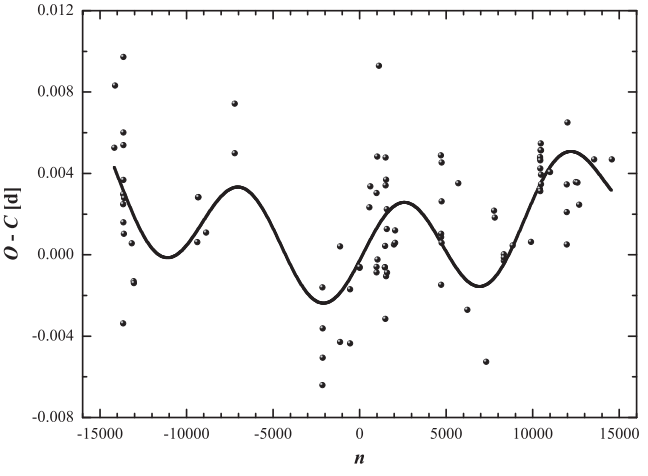

Fig. 2. The parabolic + periodic model of the *O–C* curve of ER Vul.

this pattern belongs to a periodic process. Due to the noisy character of SCD, we estimated the semi-amplitude of this periodicity by taking into account the $\Delta(O–C)$ values belonging to the interval within the minimum value and the first quartile (for estimating the minimum level), and those situated between the third quartile and the maximum value (for estimating the maximum level). Computing the corresponding weighted means, we found the semi-amplitude $\tau_{SCD} = 0.00140 \pm 0.00011\,d$. The results supplied by the two complementary methods are in good agreement (see Section 4.2 below), and consequently, this fact sustains the hypothesis concerning the reality of the inferred periodicity.

The final residuals obtained after removing the model given by Eq. (3.1) with the parameters listed in Table 1 are practically centred on zero (their mean value is $-2.8 \times 10^{-12}\,d$). They have a Gaussian distribution, according to the Kolmogorov–Smirnov test, while the application of the runs test proved their random character.

4.2. The evaluation of the detectability of the detected orbital period modulation

We applied the methodology described in Section 3.2 using the values of the parameters of the inferred periodic model given in Table 1. The number of numerical experiments was 100,000. We performed Monte Carlo simulations for amplitude of the periodic signal of the form $k_\tau \tau_{11}$, with $k_\tau < 1.0$. The amplitude value estimated from the amplitude spectrum of the *O–C* residuals after removing the parabolic trend (see Fig. 1, upper panel) is $\tau_{\max,obs} = 0.00167$ d. An equal value of the highest peak in the synthetic averaged spectrum is obtained for an "input" amplitude (see Table 1) attenuated with a factor $k_\tau = 0.577$, i.e., $k_\tau \tau_{11} = 0.00142$ d. Remark the excellent agreement between the above estimated values of τ_{SCD} and $k_\tau \tau_{11}$. This value of k_τ has to be considered from a statistical perspective: the estimated k_τ value corresponds to the most probable value of the Fourier amplitude at the frequency f_{01}^* which is equal to $\tau_{\max,obs}$ (see Fig. 4). But for lower probabilities, for other k_τ values, one may find good agreements between $\tau_{\max,obs}$ and the highest peak of amplitude spectra of other artificial time series. On the other hand, $\tau_{\max,obs}$ also represents a quantity associated to a realisation of a stochastic process: the amplitude spectrum computed on the basis of the observed timing data, which include the contributions of different noise sources related both to the observed binary system, and the observational technique as well as the data processing details. Obviously, we have no information about the actual amplitude of the involved periodic signal. Consequently, it is natural that our estimates should contain some amount of incertitude. However, this approach is able to supply a more realistic perspective on the interplay of these effects.

The "observed" spectrum and the averaged spectra generated under the two hypotheses H_0 and H_1 (Eqs. (3.2) and (3.3)) are displayed in Fig. 4. The spectrum obtained under H_0 is obviously white. The comparison between the "observed" spectrum and the averaged one reveals the persistence of some spectral features at well-defined frequencies, the most persistent being the peak situated at f_{01}^*.

The details of signal detectability evaluation relying on the number of occurrences of the highest (first order) peak in the amplitude spectra of artificial data (see Sections 3.2.1.1 and 3.2.2.2) are presented in Fig. 5. We considered the frequency interval $[0.000074, 0.000138]$ of width $\Delta f_{0w} = 0.000064$ (see Section 3.2.1.2) centred on the dominant frequency $f_{01}^* = 0.000106$.

Table 1
Parameters of the parabolic + periodic ephemeris of the timing data on ER Vul.

$t_0 = HJD2445221.10744$ ± 0.00046				
$\tau_1 \equiv P_p = 0.698094884\,dc^{-1}$ ± 0.000000037				
$\tau_2 = 1.82 \cdot 10^{-11}\,dc^{-2}$ $\pm 0.52 \cdot 10^{-11}$			$(1/P_p)(dP_p/dt) = 2.73 \cdot 10^{-8}\,\mathrm{yr}^{-1}$ $\pm 0.79 \cdot 10^{-8}$	
$f_{01} = 0.0001075$ ± 0.0000032	$P_{S1} = 17.78\,\mathrm{yr}$ ± 0.53	$\tau_{11} = 0.00246\,d$ ± 0.00048	$\Phi_{11} = 6.17\,rad$ ± 0.19	
$\sigma_{res} = 0.00257\,d$				

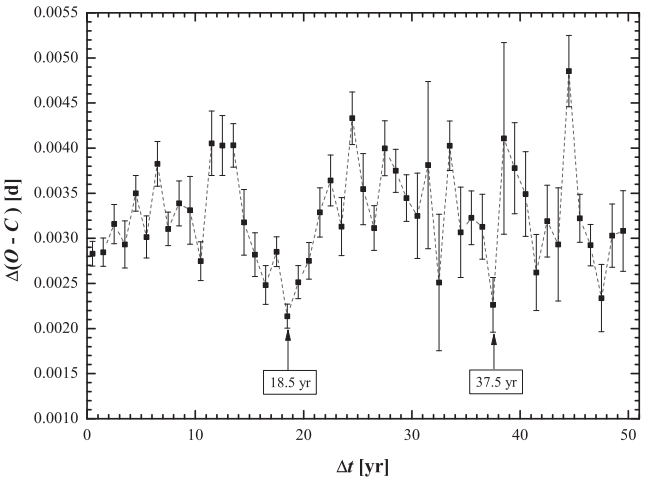

Fig. 3. The self-correlation diagram of the *O–C* residuals of ER Vul obtained after removing the parabolic trend.

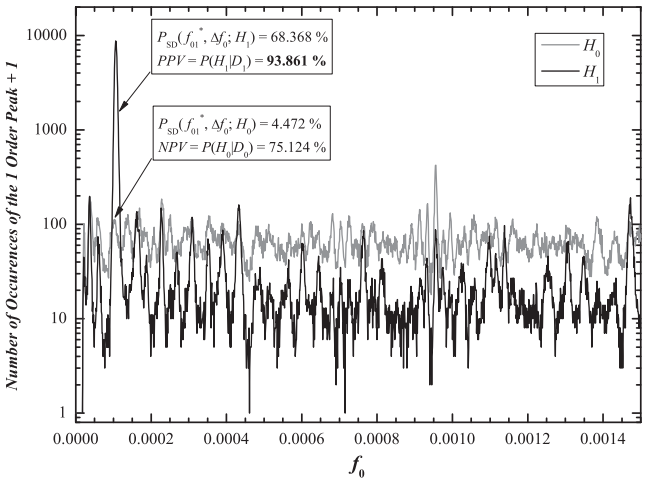

Fig. 5. Number of occurrences of the highest peak in the amplitude spectrum in the considered frequency range, for $k_\tau = 0.577$.

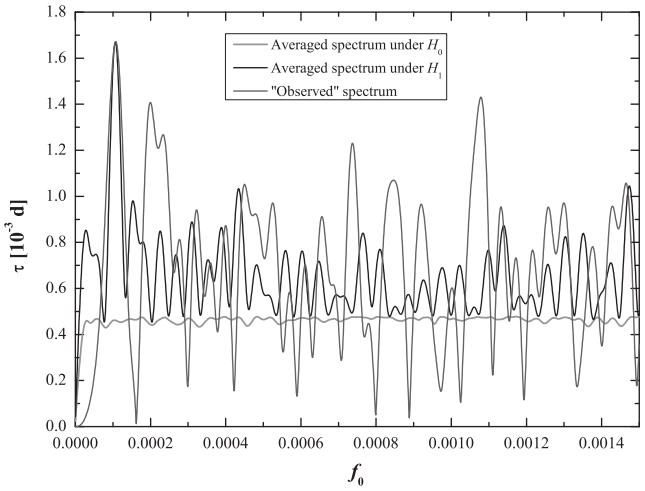

Fig. 4. Averaged artificial amplitude spectra for $k_\tau = 0.577$ together with the "observed" amplitude spectrum (identical with that plotted in Fig. 1, upper panel).

Table 2
Values of the different probabilities quantifying the detectability of the inferred orbital period modulation in the *O–C* curve of ER Vul.

Frequentist approach	Bayesian approach
$k_\tau = 1.0$	
$\tau_{max}: \alpha = 0.01025$	$\tau_{max}: P(H_0\|D_0) = 96.229\%$
$\beta = 0.03879$	$P(H_1\|D_1) = 98.945\%$
$P_{SD}(f_{01}^*, \Delta f_0; H_0) = 4.472\%$	$P(H_0\|D_0) = 97.235\%$
$P_{SD}(f_{01}^*, \Delta f_0; H_1) = 97.284\%$	$P(H_1\|D_1) = 95.605\%$
$k_\tau = 0.577$	
$\tau_{max}: \alpha = 0.01025$	$\tau_{max}: P(H_0\|D_0) = 68.121\%$
$\beta = 0.46318$	$P(H_1\|D_1) = 98.126\%$
$P_{SD}(f_{01}^*, \Delta f_0; H_0) = 4.472\%$	$P(H_0\|D_0) = 75.124\%$
$P_{SD}(f_{01}^*, \Delta f_0; H_1) = 68.368\%$	$P(H_1\|D_1) = 93.861\%$

Fig. 5 displays the histograms of the number of occurrences of the highest peak under H_0 and H_1 hypotheses, for $k_\tau = 0.577$. The corresponding values of the signal detection probability and of the posterior probabilities are also mentioned. The peak appearing at f_{01}^* under H_1 is from far the most prominent peak, its occurrence being near two magnitude orders higher than that which appeared under H_0 at the same frequency, and about 21 times higher than the highest peak which appeared under H_0.

The results of the above analyses are summarized in Table 2, in which are listed the values of different parameters featuring the detectability of the inferred periodic signal, corresponding to its observed signature: $\tau_{max,obs} = 0.00167$ d (see Fig. 1, upper panel). The results corresponding to the Bayesian approach reveals two interesting conclusions: (i) there is an excellent agreement between the values of the posterior probabilities $P(H_1|D_1)$ evaluated in case of τ_{max} (about 98.9%, and 98.1%), for the two values of k_τ, and (ii) the posterior probabilities $P(H_1|D_1)$ evaluated in case of the analysis of the dominant frequency distribution (about 95.6%, and 93.9%) also display a good agreement for the two considered values of k_τ. The overall conclusion is that the hypothesis H_1 which involves the presence of a periodic modulation of the orbital period of ER Vul may be taken into account as a working hypothesis at least. The low amplitude signal with a period of 17.78 yr proved to be possible to be detected relying on the available timing data.

4.3. The secular trend in the orbital period

The available timing data enabled us to emphasise the presence of a relatively slow increasing linear trend in the orbital period of ER Vul, which yields a concave shape of the *O–C* residuals (Fig. 2). The coefficient of the second order term proved to be statistically significant at a significance level of 0.00078. One remarks the good agreement between the values of the second order coefficient, and those of the relative period change rate corresponding to the adopted ephemerides (see Eq. (4.1), and Eq. (3.1) with Table 1). This result is in agreement with the recent inference of Nanouris et al. (2011) according to which the orbital period evolution of ER Vul is expected to be mainly driven by mass loss through stellar wind (see also Kjurkchieva et al., 2003). As we already mentioned in Section 1, this binary system is detached, and consequently this secular orbital period variation cannot be explained through the mass transfer in the system.

4.4. The third body hypothesis

Having in view the above results on periodicity analysis of the *O–C* residuals of ER Vul, we approached the interpretation of the parameters of the detected orbital period modulation phenomenon in terms of a Keplerian motion related to the presence of an unseen

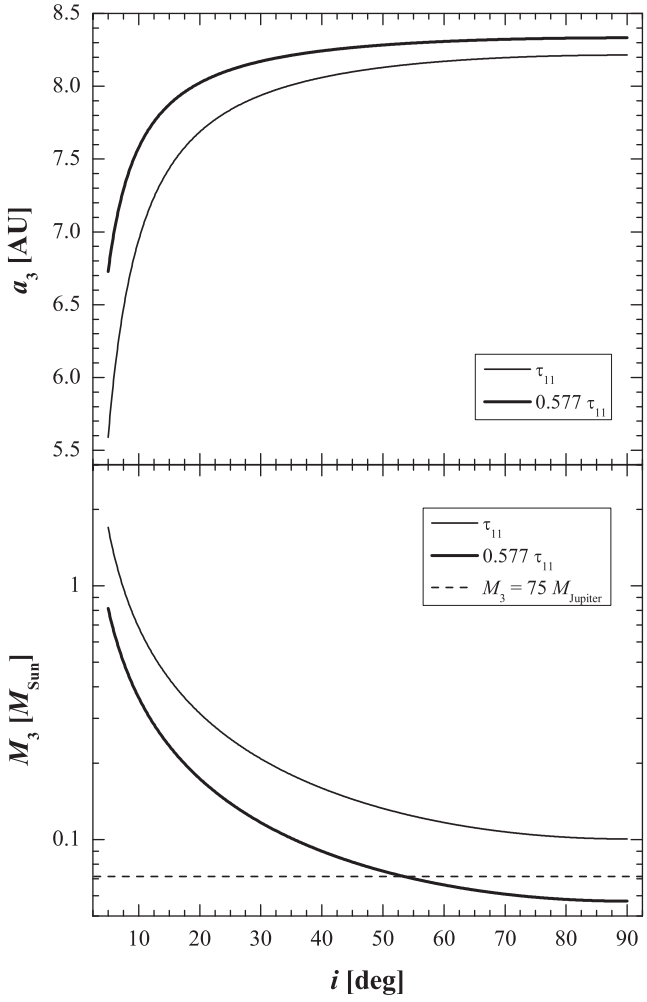

Fig. 6. The mass (lower panel) and the semimajor axis of the absolute orbit (upper panel) of the hypothetical companion for different inclination values, and for $k_\tau = 1.0$, and $k_\tau = 0.577$. The mass at which occurs the brown dwarf/main sequence cut is marked with a dashed line.

companion. Moreover, taking into account the monoperiodic character of the inferred modulation, we assumed that the hypothetical companion revolves on a circular orbit around the barycentre of the system (close binary + companion). For the detected periodicity ($P_s = 17.78$ yr), we estimated the values of the corresponding parameters: $a_{12}\sin i$ – the projection of the semimajor axis of the close binary absolute orbit on the line of sight, i – inclination of the normal to the orbit plane on the line of sight, $f(M)$ – the mass function, M_3 – the mass of the hypothetical companion, and K – the semi-amplitude of the radial velocity curve. Relying on the results of Wilson and Raichur (2011), we estimated the mass of the binary system $M_{12} = 1.939 \pm 0.021\,M_{Sun}$, with $M_1 = 0.9946 \pm 0.0108\,M_{Sun}$, and $M_2 = 0.9447 \pm 0.0113\,M_{Sun}$. Thus, for the estimated value of τ_{11} (see Table 1), we obtained: $a_{12}\sin i = 0.426\,AU$, $f(M) = 2.44 \cdot 10^{-4}\,M_{Sun} = 0.256\,M_{Jupiter}$, and $K = 0.71\,\mathrm{km\,s^{-1}}$, while for the corrected value of τ_{11}, i.e., $k_\tau\tau_{11} = 0.00142$ d, we got significantly different values of the above parameters: $a_{12}\sin i = 0.246\,AU$, $f(M) = 4.7 \cdot 10^{-5}\,M_{Sun} = 0.049\,M_{Jupiter}$, and $K = 0.41\,\mathrm{km\,s^{-1}}$. We estimated the values of the mass (M_3), and the orbit radius (a_3) of the hypothetic companion of ER Vul as functions of inclination value, for the above two considered situations (see Fig. 6). Taking into account the inclination estimated by Wilson and Raichur (2011), $i = 67.95°$, we obtained in the case of τ_{11}: $M_3 = 0.109\,M_{Sun} = 113.8\,M_{Jupiter}$, and $a_3 = 8.19\,AU$, while for $k_\tau\tau_{11}$: $M_3 = 0.062\,M_{Sun} = 64.7\,M_{Jupiter}$, and $a_3 = 8.32\,AU$. It is interesting that in case of the corrected (semi-)amplitude value of the periodic component of the O–C curve ($k_\tau\tau_{11}$), and for inclination values higher than about 53.3°, the third body in the system should be a brown dwarf ($M_3 < 75\,M_{Jupiter}$). According to the distance estimates given by Bilir et al. (2008), and Wilson and Raichur (2011), i.e., $d = 48.48 - 52.0\ pc$, we found for the minimum apparent separation of the wide system 0.062 arcsec – 0.067 arcsec, while for the maximum apparent separation we found 0.165 arcsec – 0.178 arcsec.

We investigated the stability of the two hypothetical triple systems in the frame of the two-body approximation using the simple stability criterion of Szebehely and Zare (1977). The coplanarity of the orbits of the inner close binary system (ER Vul) and wide system (close binary + companion) is obviously assumed. It resulted that in both cases (τ_{11}, and $k_\tau\tau_{11}$) the respective triple systems would be stable either for direct or retrograde motion, but "more stable" in case of direct motion.

4.5. The magnetic activity cycles hypothesis

As we already mentioned in Section 1, both component stars of ER Vul display intense stellar activity and therefore a modulation of the orbital period induced by the cyclic magnetic activity is to be expected to occur (e.g., Hall, 1989, 1990). The mechanism used to explain such a phenomenon, and also to investigate its implications, i.e., to estimate the values of some specific physical parameters, is that proposed by Applegate (1992), which was further investigated by Lanza et al. (1998), Lanza and Rodonò (1999), and Lanza (2005). From the beginning we have to remind that this approach relies on a well-defined model for the considered binary system: it consists of a magnetically active star and a companion star which has no magnetic activity, and which can be regarded as a point mass. Consequently, having in view that both components of ER Vul have late spectral types G1-2 V + G3 V, and are magnetically active (Duemmler et al., 2003), Applegate's (1992) model is not suitable to be applied in this case.

However, for the two amplitudes of the periodic term (τ_{11} and $k_\tau\tau_{11}$), we computed some overall parameters (e.g., Applegate, 1992; Lanza and Rodonò, 1999) for the component stars of the system: A_{O-C} – the semi-amplitude of the O–C curve, $\Delta P_p/P_p$ – the relative semi-amplitude of the orbital period modulation, ΔQ – the variation of the quadrupole moment of the active star which would be related to the observed $\Delta P_p/P_p$ value. The following values have been obtained for these parameters (the orbital period is $P_S = 17.78$ yr, see Table 1):

- $A_{O-C} = \tau_{11} = 0.00246$ d,

$$\Delta P_p/P_p = 2.38 \times 10^{-6},\ \Delta Q_1 = -4.31 \times 10^{42}\ \mathrm{kg\,m^2},\ \Delta Q_2 = -4.10 \times 10^{42}\ \mathrm{kg\,m^2},$$

- $A_{O-C} = 0.577\,\tau_{11} = 0.00142$ d,

$$\Delta P_p/P_p = 1.37 \times 10^{-6},\ \Delta Q_1 = -2.49 \times 10^{42}\ \mathrm{kg\,m^2},\ \Delta Q_2 = -2.36 \times 10^{42}\ \mathrm{kg\,m^2}.$$

The $\Delta P_p/P_p$ values obtained for the two considered O–C curve (semi-) amplitudes are typical for W UMa systems. This result is in agreement with the evolutionary stage of ER Vul (see Section 1). The ΔQ values for the two component stars are of the same order of magnitude with those computed for other W UMa systems, e.g., AB And (Borkovits et al., 2005), and CK Boo (Pop and Vamoş, 2012), or for cataclysmic variables (e.g., Lanza and Rodonò, 1999).

We also remark that the periodicity found by us (17.78 yr) significantly differs from the prediction relying on the correlation

suggested by Lanza and Rodonò (1999) (27.9 or 26.6 yr; see Section 1). It does not necessarily mean that the orbital modulation mechanism could not involve the cyclic magnetic activity of the component stars of ER Vul, but it is another reason to deepen the study of this correlation.

An interesting approach to explain the orbital period modulation in magnetically active close binaries has been proposed by Yuan and Qian (2007). In their model, the authors take into account the magnetic connexion of the binary system components, when their separation is very small, i.e., $a/(R_1 + R_2) \approx 1$–3, and consequently, the stars will magnetise each other. Making some simplifying assumptions, Yuan and Qian (2007) succeed to derive analytic formulae for the magnetic field inside the two component stars, and for the mean magnetic field that we can observe. Given the above mentioned characteristics of ER Vul (both components are magnetically active, and $a/(R_1 + R_2) = 1.9$), this model can be applied for this binary system. We computed the following estimates for the above magnetic fields:

- $A_{O-C} = \tau_{11}$: $B_0 = 75.1$ T, $\overline{B}_s = 6.0 - 9.0$ T,
- $A_{O-C} = 0.577\,\tau_{11}$: $B_0 = 57.0$ T, $\overline{B}_s = 4.6 - 6.8$ T.

These values are in relatively good agreement with the estimates given by Yuan and Qian (2007) in their Table 1. It is interesting to remark that the above $\overline{B}_s$ values are also in agreement with the values of mean magnetic field involved in the model of Lanza et al. (1998) (1–6 T).

5. Concluding remarks

The orbital period variability of the close binary system ER Vul has been reanalyzed relying on 91 times of primary and secondary minimum light which cover a time base of about 54.9 yr. We found that the run of the *O–C* residuals can be described by a statistically significant secular parabolic trend corresponding to a relatively slow increasing trend in the orbital period featured by a relative period change rate of $2.73 \times 10^{-8}\,\mathrm{yr}^{-1}$, and a 17.78 yr periodic component, with a low amplitude of about 3.5 min. Although the confidence level for the rejection of the null hypothesis (a little over 96%) was lower than the threshold usually taken into account (99.9%), we decided to claim the detection of this periodic signal because of its confirmation through the complementary method of self-correlation analysis. However, having in view the rather subliminal character of this modulation, we approached the problem of evaluation the detectability of such signal.

We have estimated our chance to detect a signal having the same parameters as those estimated, in data sets consisting in the same amount of data, the same sampling, and the same noise level as that estimated (assuming a Gaussian distribution). We proposed two complementary methodologies based on binary decision making relying on Monte Carlo simulations intended for detectability evaluation of periodic signals in the presence of high level additive noise. For each of them we gave both frequentist and Bayesian approaches. The latter supplied the most consistent and also optimistic results.

The application of these methodologies supplied us consistent results (see Table 2) and lead us to conclude that the inferred orbital period modulation phenomenon may be real. An additional and important conclusion was that the actual amplitude of the signal is lower (≈2.0 min) than that estimated by us through the usual data modelling technique. It has direct implications for a realistic physical interpretation of the observed modulation phenomenon. At this moment, in case of ER Vul it is difficult to give a definite answer to this problem. Both considered mechanisms, light-time effect due to the presence of an unseen companion (a low mass star or even a relatively high mass brown dwarf), and the magnetic activity cycles of the component stars seem plausible.

Obviously, the results of the present study of the orbital period variability of ER Vul need further observational confirmation. New, high quality timing and radial velocity data will be necessary for this reason. Long time base and precise photometric data with high temporal resolution are also required in order to investigate the possible influence of light curve distortions and rapid variability (see Section 1) on the estimation of the times of minima, and thus, their influence on the shape of *O–C* curve. Furthermore, the development of a new model to explain orbital period modulation by magnetic cycles occurring in close binary systems whose both components are active (see also Lanza, 2005) will be extremely important for discriminating between different possible mechanisms.

References

Applegate, J.H., 1992. ApJ 385, 621.
Appourchaux, T., 2011. arXiv:1103.5352v2 [astro-ph.IM].
Axelsson, S., 1999. The base-rate fallacy and its implications for the difficulty of intrusion detection. In: Proceedings of the 6th ACM Conference on Computer and Communications Security (CCS '99). Kent Ridge Digital Labs, Singapore, pp. 1–7.
Bilir, S., Ak, T., Soydugan, E., Soydugan, F., Yaz, E., Filiz Ak, N., Eker, Z., Demircan, O., Helavci, M., 2008. AN 329, 835.
Borkovits, T., Elkhateeb, M.M., Csizmadia, Sz., Nuspl, J., Bíró, I.B., Hegedüs, T., Csorvási, R., 2005. A&A 441, 1087.
Çakirli, Ö., İbanoğlu, C., Fraska, A., Catalano, S., 2003. A&A 400, 257.
Deeming, T.J., 1975. Ap&SS 36, 137.
Dryomova, G., Perevozkina, E., Svechnikov, M., 2005. A&A 437, 375.
Duemmler, R., Doucet, C., Formanek, F., Ilyin, I., Tuominen, I., 2003. A&A 402, 745.
Ekmekçi, F., Özeren, F.F., Ak, H., 2002. AN 323, 31.
Fawcett, T., 2006. Pattern Recogn. Lett. 27, 861.
Gunn, A.G., Doyle, J.G., 1997. A&A 318, 60.
Hall, D.S., 1976. The RS CVn binaries and binaries with similar properties. In: Fitch, W. (Ed.), Multiple Periodic Variable Stars. Reidel, Dordrecht, pp. 287–348.
Hall, D.S., 1989. SSR 50, 219.
Hall, D.S., 1990. Period changes and magnetic cycles. In: İbanoğlu, C. (Ed.), Active Close Binaries. Kluwer Academic Publishers, Dordrecht, pp. 95–119.
Harmanec, P., Božić, H., Thanjavour, K., Robb, R.M., Ruždjak, D., Sudar, D., 2004. A&A 415, 289.
İbanoğlu, C., Evren, S., Akan, M.C., Tunca, Z., Keskin, V., 1993. A&A 269, 310.
Kalimeris, A., Rovithis-Livaniou, H., Rovithis, P., 1994. A&A 282, 775.
Kjurchieva, D.P., Marchev, D.V., Zola, S., 2003. A&A 404, 611.
Lanza, A.F., 2005. MNRAS 364, 238.
Lanza, A.F., Rodonò, M., 1999. A&A 349, 887.
Lanza, A.F., Rodonò, M., Rosner, R., 1998. MNRAS 296, 893.
Liao, W.-P., Qian, S.-B., 2010. MNRAS 405, 1930.
Liteanu, C., Rîcă, I., 1985. Optimizarea proceselor analitice. Editura Academiei Republicii Socialiste România, Bucureşti.
Mennella, V., 1990. A&A 234, 203.
Milano, L., Mancuso, S., Vittone, A., D'Orsi, A., Marcozzi, S., 1986. Ap&SS 124, 83.
Nanouris, N., Kalimeris, A., Antonopoulou, E., Rovithis-Livaniou, H., 2011. A&A 535, 1–11.
Northcott, R.J., Bakos, G.A., 1967. AJ 72, 89.
Oláh, K., Budding, E., Kim, H.-I., Etzel, P., 1994. A&A 291, 110.
Percy, J.R., Hosick, J., Leigh, N.W.C., 2003. PASP 115, 59.
Percy, J.R., Jakate, S.M., Matthews, J.M., 1981. AJ 86, 53.
Percy, J.R., Ralli, J.A., Sen, L.V., 1993. PASP 105, 287.
Pohl, E., Evren, S., Tümer, O., Sezer, C., 1982. IBVS, No. 2189.
Pop, A., 1999. IBVS, No. 4801.
Pop, A., 2005. On the orbital period modulation of the eclipsing binary system Y Leonis. In: Sterken, C. (Ed.), The Light-Time Effect in Astrophysics. ASP Conf. Ser., pp. 263–268, vol. 335.
Pop, A., 2007. Romanian Astron. J. 17, 35.
Pop, A., Bărbosu, M., 2006. Romanian Astron. J. 16, 179–183.

Pop, A., Vamoş, C., 2007. Romanian Astron. J. 17, 101.
Pop, A., Vamoş, C., 2012. NewA 17, 667.
Pop, A., Liteanu, V., Moldovan, D., 2003. Ap&SS 284, 1207.
Pop, A., Turcu, V., Marcu, A., 2011. Ap&SS 333, 17.
Pop, A., Vamoş, C., Turcu, V., 2010. AJ 139, 425.
Press, W.H., Rybicki, G.B., 1989. ApJ 338, 277.
Qian, S.B., 2001. Possible magnetic activity cycles of four chromospherically active binaries: ER Vul, UV Psc, AR Lac and BH Vir. In: Brekke, P., Fleck, B., Gurman, J.B. (Eds.), Proc. IAU Symposium, 203, Recent Insights into the Physics of the Sun and Heliosphere: Highlights from SOHO and Other Space Missions, pp. 437–440.
Qian, S., Liu, Q., Yang, Y., 1998. Ap&SS 257, 1.
Roberts, D.H., Lehár, J., Dreher, J.W., 1987. AJ 93, 968.
Samolyk, G., 2012. JAAVSO 40, 975.
Scargle, J.D., 1982. ApJ 263, 835.
Shkolnik, E., Walker, G.A.H., Rucinski, S.M., Bohlender, D.A., Davidge, T.J., 2005. AJ 130, 799.
Srivastava, R.K., Padalia, T.D., Srivastava, J.B., 1991. Ap&SS 182, 281.
Sturrock, P.A., Scargle, J.D., 2009. ApJ 706, 393.
Szebehely, V., Zare, K., 1977. A&A 58, 145.
Welsh, W.F., 1997. Measuring variability in the presence of noise. In: Maoz, D., Sternberg, A., Leibowitz, E.M. (Eds.), Astronomical Time Series, Astrophysics and Space Science Library. Kluwer Academic Publishers, Dordrecht, pp. 171–174, vol. 218.
Wilson, R.E., Raichur, H., 2011. MNRAS 415, 596.
Yuan, J., Qian, S., 2007. ApJ 669, L93.
Zeinali, F., Edalati, M.T., Mirtorabi, M.T., 1995. IBVS, No. 4190.
Zwintz, K., Weiss, W.W., Kuschnig, R., Gruber, R., Frandsen, S., Gray, R., Jenkner, H., 2000. A&AS 145, 481.